IOPscience iopscience.iop.org

Home Search Collections Journals About Contact us My IOPscience

Ion-acoustic waves in a two-electron-temperature plasma: oblique modulation and envelope excitations

This article has been downloaded from IOPscience. Please scroll down to see the full text article.

2003 J. Phys. A: Math. Gen. 36 11901

(http://iopscience.iop.org/0305-4470/36/47/015)

View the table of contents for this issue, or go to the journal homepage for more

Download details:
IP Address: 171.66.16.89
The article was downloaded on 02/06/2010 at 17:17

Please note that terms and conditions apply.

INSTITUTE OF PHYSICS PUBLISHING JOURNAL OF PHYSICS A: MATHEMATICAL AND GENERAL

J. Phys. A: Math. Gen. **36** (2003) 11901–11913 PII: S0305-4470(03)65563-0

Ion-acoustic waves in a two-electron-temperature plasma: oblique modulation and envelope excitations

I Kourakis[1] **and P K Shukla**

Institut für Theoretische Physik IV, Fakultät für Physik und Astronomie, Ruhr-Universität Bochum, D-44780 Bochum, Germany

E-mail: ioannis@tp4.rub.de and ps@tp4.rub.de

Received 1 July 2003
Published 12 November 2003
Online at stacks.iop.org/JPhysA/36/11901

Abstract

Theoretical and numerical studies are carried out for the nonlinear amplitude modulation of ion-acoustic waves propagating in an unmagnetized, collisionless, three-component plasma composed of inertial positive ions moving in a background of two thermalized electron populations. Perturbations oblique to the carrier wave propagation direction have been considered. The stability analysis, based on a nonlinear Schrödinger-type equation, shows that the wave may become unstable; the stability criteria depend on the angle θ between the modulation and propagation directions. Different types of localized excitations (envelope solitary waves) are shown to exist, in qualitative agreement with satellite observations in the magnetosphere.

PACS numbers: 52.35.Fp, 52.35.Mw, 52.35.Sb

1. Introduction

Ion-acoustic waves (IAW) are well-known electrostatic plasma modes [1], where a population of inertial ions oscillate against a dominant thermalized background of electrons providing the necessary restoring force. The IAW phase velocity lies between the electron and ion thermal velocities.

The linear properties of the IA wave have been extensively studied and well understood since a long time ago. As far as nonlinear effects are concerned, the formation of IAW-related localized structures, due to the mutual compensation between nonlinearity and dispersion, when physically possible, has been anticipated theoretically, either via the Korteweg–deVries (KdV) or Zakharov–Kuznetsov (ZK) equation [2, 3], describing small amplitude

[1] On leave from: ULB—Université Libre de Bruxelles, Faculté des Sciences Apliquées, CP 165/81 Physique Générale, Avenue F D Roosevelt 49, B-1050 Brussels, Belgium.

 © 2003 IOP Publishing Ltd Printed in the UK

solitary waves, or the Sagdeev potential formalism [4–7], accounting for arbitrary amplitude excitations, and also experimentally confirmed [8].

The amplitude modulation of waves propagating in nonlinear dispersive media is a unique nonlinear phenomenon that is relevant to many areas including physics and technology. For large amplitude waves interacting with background media, nonlinear harmonic generation due to carrier wave self-interaction comes into the picture. Self-modulation involving second harmonic generation is responsible for modulational instabilities and possibly energy localization via the formation of envelope excitations (solitons). This rather ubiquitous mechanism has been studied in a wide variety of physical contexts, ranging from nonlinear optics [9–14] and solid state physics [15] to hydrodynamics [16], plasma physics [17] and even Bose–Einstein condensation [18, 19]; applications also include signal transmission lines [16, 20], fibre telecommunications [21] and charge transport in molecular systems [22]. The standard method consists in using a reductive perturbation (multiple spatio-temporal scales) technique [23], which allows one to derive a nonlinear Schrödinger-type (NLS) equation [24] for the modulated wave envelope from the relevant governing equations describing the physical system considered. Regarding the propagation of electrostatic plasma waves, this formalism has been applied in studies of ion-acoustic waves [23, 25–29], and theoretical predictions have been experimentally confirmed [30]. The ion-acoustic mode, yet initially shown to be stable to parallel modulation (for long wavelengths λ much larger than the Debye length λ_D) [25], was later shown to be modulationally unstable for wavelengths above a wavenumber threshold of k_{cr} ($\approx 1.47\, 2\pi/\lambda_D$) [26]. The IAW instability region was shown to depend strongly on the ion temperature [27] and obliqueness in modulation [28] and, eventually, the Landau damping mechanism, which operates at small wavelength modes [29].

The characteristics of the IAW propagation can be strongly modified by the existence of a minority population of 'cold' (yet still Maxwellian) electrons, as has been shown theoretically [3, 5, 6, 31, 32] and experimentally [31, 33]. Regarding applications, it may be noted that the injection of cold electrons into a plasma and the subsequent decrease of the phase speed of waves has been suggested as a possible IAW stabilization mechanism, as well as an ion heating enhancement method [31].

Interestingly, studies of two-electron-temperature plasmas are encouraged by satellite observations of moving localized potential variation regions, reported by recent spacecraft missions e.g. the FAST at the auroral region [34, 35], as well as the S3-3 [36], Viking [37],[2] GEOTAIL and POLAR [35, 38] earlier missions in the magnetosphere, where such an electron population coexistence is encountered. Some of the localized structures reported therein bear qualitative characteristics which are reminiscent of solitary electrostatic waves and are strongly believed to be related to ion-acoustic waves (see the discussion in [35]). It should be stressed that both compressive and rarefactive large amplitude structures have been observed [34]. Furthermore, it has recently been suggested [35] that neither the velocity dependence of the observed potential structure amplitudes nor their asymmetry should be taken for granted, since they may be attributed to intrinsic measurement errors. Finally, the observed phase speeds lie over an extended region of values, sometimes even above the ion sound speed; these facts seem to suggest that plainly employing the KdV picture may not suffice for the elucidation of the generation of these solitary structures and an alternative instability mechanism may be present (also see the discussion in [32, 35]).

In this paper, we study the occurrence of modulational instability, as well as the existence of envelope solitary structures, related to ion-acoustic waves propagating in a collisionless

[2] The interpretation of the Viking measurements [37] has recently risen some doubt (see the thorough discussion in [35]).

unmagnetized plasma consisting of three distinct particle species 's': an inertial species of ions (denoted by 'i'; mass m_i, charge $q_\mathrm{i} = +Z_\mathrm{i}e$), surrounded by an environment of two populations of (thermalized) electrons (mass m_e, charge e), at different temperatures T_h and T_c (for 'hot' and 'cold', respectively). Charge neutrality is assumed at equilibrium.

2. The model equations

Let us consider the moment—Poisson system of equations for the ions. The (number) density n_i is governed by the (continuity) equation

$$\frac{\partial n_\mathrm{i}}{\mathrm{d}t} + \nabla \cdot (n_\mathrm{i}\mathbf{u}_\mathrm{i}) = 0 \tag{1}$$

and the mean velocity $\mathbf{u}_\mathrm{i}$ obeys

$$\frac{\partial \mathbf{u}_\mathrm{i}}{\mathrm{d}t} + \mathbf{u}_\mathrm{i} \cdot \nabla \mathbf{u}_\mathrm{i} = -\frac{Z_\mathrm{i}e}{m_\mathrm{i}}\nabla\Phi \tag{2}$$

where Φ is the electrostatic potential. The system is closed with Poisson's equation

$$\nabla^2\Phi = -4\pi \sum q_\mathrm{s}n_\mathrm{s} = 4\pi e(n_\mathrm{c} + n_\mathrm{h} - Z_\mathrm{i}n_\mathrm{i}) \tag{3}$$

where we assume a nearly Maxwellian distribution for the electrons i.e. $n_\mathrm{h/c} \approx n_\mathrm{h/c_0} e^{e\Phi/k_\mathrm{B}T_\mathrm{h/c}}$ ($T_\mathrm{h/c}$ is the hot/cold electron temperature, k_B is the Boltzmann constant). The right-hand side cancels at equilibrium due to the overall neutrality condition

$$n_\mathrm{c,0} + n_\mathrm{h,0} - Z_\mathrm{i}n_\mathrm{i,0} = 0. \tag{4}$$

By using this 'cold ion' model as a first step, we have neglected the ion temperature effect, which we have left for a forthcoming study.

Choosing appropriate physical scales, one may normalize all quantities and develop around equilibrium, i.e. $\Phi \approx 0$. First, let us define the effective electron temperature $T_\mathrm{eff} = (n_\mathrm{h,0} + n_\mathrm{c,0})/(n_\mathrm{h,0}/T_\mathrm{h} + n_\mathrm{c,0}/T_\mathrm{c})$ and the 'effective sound speed' $c_\mathrm{s,eff} = (Z_\mathrm{i}k_\mathrm{B}T_\mathrm{eff}/m_\mathrm{i})^{1/2}$, in agreement with previous experimental [31] and theoretical [32] considerations. Note that, interestingly, the effective electron temperature T_eff remains finite, even if the hot electron temperature T_h tends to infinity (in the presence of even a small percentage of cold electron population) as pointed out in [31]. Let us now scale time and space over the ion plasma period $\omega_\mathrm{p,i}^{-1} = \left(4\pi n_\mathrm{i,0}Z_\mathrm{i}^2e^2/m_\mathrm{e}\right)^{-1/2}$ and the effective Debye length $\lambda_\mathrm{D,eff} = (k_\mathrm{B}T_\mathrm{eff}/4\pi Z_\mathrm{i}n_\mathrm{i,0}e^2)^{1/2} \equiv c_\mathrm{s,eff}/\omega_\mathrm{p,i}$, respectively. Equations (1)–(4) can thus be combined into the reduced equations

$$\frac{\partial n}{\mathrm{d}t} + \nabla \cdot (n\mathbf{u}) = 0$$
$$\frac{\partial \mathbf{u}}{\mathrm{d}t} + \mathbf{u} \cdot \nabla \mathbf{u} = -\nabla\phi$$

and

$$\nabla^2\phi = 1 + \phi + \alpha\phi^2 + \alpha'\phi^3 - n \tag{5}$$

where all quantities are non-dimensional: $n = n_\mathrm{i}/n_\mathrm{i,0}$, $\mathbf{u} = \mathbf{u}_\mathrm{i}/v_0$ and $\phi = \Phi/\Phi_0$; the scaling quantities are, respectively: the equilibrium ion density $n_\mathrm{i,0}$, the 'effective sound speed' $v_0 = c_\mathrm{s,eff}$ (defined above) and $\Phi_0 = (k_\mathrm{B}T_\mathrm{eff}/e)$. The dimensionless parameters α, α' in the last equation are given by

$$\alpha = \frac{1}{2}(n_\mathrm{c,0} + n_\mathrm{h,0})\frac{\frac{n_\mathrm{c,0}}{T_\mathrm{c}^2} + \frac{n_\mathrm{h,0}}{T_\mathrm{h}^2}}{\left(\frac{n_\mathrm{c,0}}{T_\mathrm{c}} + \frac{n_\mathrm{h,0}}{T_\mathrm{h}}\right)^2} = \frac{1}{2}(1+\nu)\frac{\nu + \mu^2}{(\nu+\mu)^2}$$

$$\alpha' = \frac{1}{6}(n_{\mathrm{c},0}+n_{\mathrm{h},0})^2 \frac{\frac{n_{\mathrm{c},0}}{T_{\mathrm{c}}^3}+\frac{n_{\mathrm{h},0}}{T_{\mathrm{h}}^3}}{\left(\frac{n_{\mathrm{c},0}}{T_{\mathrm{c}}}+\frac{n_{\mathrm{h},0}}{T_{\mathrm{h}}}\right)^3} = \frac{1}{6}(1+\nu)^2\frac{\nu+\mu^3}{(\nu+\mu)^3}$$

where we defined the hot-to-cold electron density and temperature ratio, namely $\nu = n_{\mathrm{h},0}/n_{\mathrm{c},0}$ and $\mu = T_{\mathrm{h}}/T_{\mathrm{c}}$, respectively. Note that, taking the isothermal limit $\nu \to 0$ (or $\nu \to \infty$ or $\mu \to 1$), one recovers exactly the 'ordinary' IAW (e–i plasma) values $\alpha' = \frac{2}{3}\alpha^2 = \frac{1}{6}$ [25, 26], while in the limit $\mu \to \infty$, one obtains: $\alpha' = \frac{2}{3}\alpha^2 = \frac{1}{6}(1+\nu)^2$. The parameters ν and μ rather generally (yet not exclusively) bear values above unity; typical experimental values e.g. in rf discharge experiments: $\mu = 14, \mu = 12.6$ [33] are of similar order of magnitude as those reported in satellite observations: typically $T_{\mathrm{h}} = 10\,\mathrm{eV}$, $T_{\mathrm{c}} = 0.8\,\mathrm{eV}$, i.e. $\mu = 12.5$ and $\nu = 10$ [37] or even possibly higher [32]. Lower experimental values, i.e. μ between 2 and 5 and ν varying from $1/6$ to 3, have also been reported in discharge plasmas [31].

3. Perturbative analysis

Let S be the state (column) vector $(n, \mathbf{u}, \phi)^{\mathrm{T}}$, describing the system's state at a given position $\mathbf{r}$ and instant t. Small deviations will be considered from the equilibrium state $S^{(0)} = (1, \mathbf{0}, 0)^{\mathrm{T}}$ by taking $S = S^{(0)} + \epsilon S^{(1)} + \epsilon^2 S^{(2)} + \cdots = S^{(0)} + \sum_{n=1}^{\infty} \epsilon^n S^{(n)}$, where $\epsilon \ll 1$ is a smallness parameter. Following the standard multiple scale (reductive perturbation) technique [23], we may consider a set of stretched (slow) space and time variables $\zeta = \epsilon(x - \lambda t)$ and $\tau = \epsilon^2 t$, where λ is to be later determined by compatibility requirements. All perturbed states depend on the fast scales via the phase $\theta_1 = \mathbf{k}\cdot\mathbf{r} - \omega t$ only, while the slow scales only enter the lth harmonic amplitude $S_l^{(n)}$, namely $S^{(n)} = \sum_{l=-\infty}^{\infty} S_l^{(n)}(\zeta,\tau)\,\mathrm{e}^{\mathrm{i}l(\mathbf{k}\cdot\mathbf{r}-\omega t)}$; the reality condition $S_{-l}^{(n)} = S_l^{(n)*}$ is met by all state variables. Two directions are therefore of importance in this (three dimensional) problem: the (arbitrary) propagation direction and the oblique modulation direction, defining, say, the x-axis, characterized by an angle variable θ. The wavenumber vector $\mathbf{k}$ is thus taken to be $\mathbf{k} = (k_x, k_y) = (k\,\cos\theta, k\,\sin\theta)$.

Substituting the above expressions into the system of equations (5) and isolating distinct orders in ϵ, we obtain the nth-order reduced equations

$$-\mathrm{i}l\omega n_l^{(n)} + \mathrm{i}l\mathbf{k}\cdot\mathbf{u}_l^{(n)} - \lambda\frac{\partial n_l^{(n-1)}}{\partial\zeta} + \frac{\partial n_l^{(n-2)}}{\partial\tau} + \frac{\partial u_{l,x}^{(n-1)}}{\partial\zeta} + \sum_{n'=1}^{\infty}\sum_{l'=-\infty}^{\infty}\left[\mathrm{i}l\mathbf{k}\cdot\mathbf{u}_{l-l'}^{(n-n')}n_{l'}^{(n')} + \frac{\partial}{\partial\zeta}\left(n_{l'}^{(n')}u_{(l-l'),x}^{(n-n'-1)}\right)\right] = 0 \tag{6}$$

$$-\mathrm{i}l\omega\mathbf{u}_l^{(n)} + \mathrm{i}l\mathbf{k}\phi_l^{(n)} - \lambda\frac{\partial\mathbf{u}_l^{(n-1)}}{\partial\zeta} + \frac{\partial\mathbf{u}_l^{(n-2)}}{\partial\tau} + \frac{\partial\phi_l^{(n-1)}}{\partial\zeta}\hat{x} + \sum_{n'=1}^{\infty}\sum_{l'=-\infty}^{\infty}\left[\mathrm{i}l'\mathbf{k}\cdot\mathbf{u}_{l-l'}^{(n-n')}\mathbf{u}_{l'}^{(n')} + u_{(l-l'),x}^{(n-n'-1)}\frac{\partial\mathbf{u}_{l'}^{(n')}}{\partial\zeta}\right] \tag{7}$$

and

$$n_l^{(n)} - (l^2k^2+1)\phi_l^{(n)} + 2\,\mathrm{i}lk_x\frac{\partial\phi_l^{(n-1)}}{\partial\zeta} + \frac{\partial^2\phi_l^{(n-2)}}{\partial\zeta^2} - \alpha\sum_{n'=1}^{\infty}\sum_{l'=-\infty}^{\infty}\phi_{l-l'}^{(n-n')}\phi_{l'}^{(n')} - \alpha'\sum_{n',n''=1}^{\infty}\sum_{l',l''=-\infty}^{\infty}\phi_{l-l'-l''}^{(n-n'-n'')}\phi_{l'}^{(n')}\phi_{l''}^{(n'')} = 0. \tag{8}$$

For convenience, in calculation one may consider, instead of the vectorial relation (7), the scalar one obtained by taking its scalar product with the wavenumber **k**.

The standard perturbation procedure now consists in solving in successive orders $\sim\epsilon^n$ and substituting in subsequent orders. For instance, the equations for $n = 2, l = 1$

$$-\mathrm{i}l\omega n_l^{(1)} + \mathrm{i}l\mathbf{k}\cdot\mathbf{u}_l^{(1)} = 0 \tag{9}$$

$$-\mathrm{i}l\omega \mathbf{u}_l^{(1)} + \mathrm{i}l\mathbf{k}\phi_l^{(1)} = 0 \tag{10}$$

and

$$n_l^{(1)} - (l^2k^2 + 1)\phi_l^{(1)} = 0 \tag{11}$$

provide the familiar IAW dispersion relation

$$\omega^2 = \frac{k^2}{k^2+1} \tag{12}$$

i.e. restoring dimensions

$$\omega^2 = \omega_{\mathrm{p,i}}^2 \frac{k^2}{k^2 + k_{\mathrm{D}}^2} \equiv \frac{c_{\mathrm{s}}^2 k^2}{1 + k^2 \lambda_{D_{\mathrm{eff}}}^2} \tag{13}$$

and determine the first harmonics of the perturbation, namely

$$\begin{aligned} n_1^{(1)} &= (1+k^2)\phi_1^{(1)} \qquad & \mathbf{k}\cdot\mathbf{u}_1^{(1)} &= \omega n_1^{(1)} \\ u_{1,x}^{(1)} &= \frac{\omega}{k}\cos\theta n_1^{(1)} \qquad & u_{1,y}^{(1)} &= \frac{\omega}{k}\sin\theta n_1^{(1)}. \end{aligned} \tag{14}$$

Proceeding in the same manner, we obtain the second-order quantities, namely the amplitudes of the second harmonics $S_2^{(2)}$ and constant ('direct current') terms $S_0^{(2)}$, as well as a non-vanishing contribution $S_1^{(2)}$ to the first harmonics. The lengthy expressions for these quantities, omitted here for brevity, are conveniently expressed in terms of the first-order potential correction $\phi_1^{(1)}$. The equations for $n = 2, l = 1$ then provide the compatibility condition: $\lambda = v_g(k) = \frac{\partial\omega}{\partial k_x} = \omega'(k)\cos\theta = \frac{\omega^3}{k^3}\cos\theta$; λ is therefore the group velocity in the x direction.

4. A nonlinear Schrödinger equation

Proceeding to the third order in ϵ ($n = 3$), the equations for $l = 1$ yield an explicit compatibility condition in the form of the NLS equation

$$\mathrm{i}\frac{\partial\psi}{\partial\tau} + P\frac{\partial^2\psi}{\partial\zeta^2} + Q|\psi|^2\psi = 0. \tag{15}$$

The 'slow' variables $\{\zeta, \tau\}$ were defined above.

The *dispersion coefficient* P is related to the curvature of the dispersion curve as $P = \frac{1}{2}\frac{\partial^2\omega}{\partial k_x^2} = \frac{1}{2}\left[\omega''(k)\cos\theta + \omega'(k)\frac{\sin^2\theta}{k}\right]$; the exact form of P reads

$$P(k) = \frac{1}{2\omega}\left(\frac{\omega}{k}\right)^4 [1 - (1+3\omega^2)\cos^2\theta]. \tag{16}$$

Note that expressions (12) and (16) above are identical to IAW quantities derived earlier, e.g. expressions (3) and (4) in [28]. Therefore, no effect is observed on the linear wave dispersion laws, due to the existence of the two electron populations (see that both parameters ν, τ are absent in the preceding formulae). It seems appropriate to point out the effect of the oblique modulation on the sign of P. The dispersion coefficient P is readily seen to be negative for parallel modulation, i.e. taking $\theta = 0$; however, for $\theta \neq 0$ this is no longer the case, since

P changes sign at some critical value of k. This fact has been pointed out (in the e–i plasma case) in [28].

The *nonlinearity coefficient* Q is due to the carrier wave self-interaction. Distinguishing different contributions, Q can be split into three distinct parts, namely $Q = Q_0 + Q_1 + Q_2$, where

$$Q_0 = +\frac{1}{2\omega}\frac{\omega^4}{k^4}\frac{1}{1-v_g^2}\left\{k^2\left[3+6k^2+4k^4+k^6-2\alpha\left(2k^2+3-2\alpha v_g^2\right)\right.\right.$$
$$\left.+(2+4k^2+3k^4+k^6-2\alpha)\cos 2\theta\right]+2(1+k^2)^4\omega^2\cos^2\theta$$
$$\left.+2k^3(1+k^2)\frac{v_g}{\omega}(1+k^2-2\alpha)\cos\theta\right\} \tag{17}$$

$$Q_1 = \frac{3\alpha'}{2}\frac{\omega^3}{k^2} \tag{18}$$

$$Q_2 = -\frac{1}{12\omega}\frac{\omega^4}{k^4}\{2[-5\alpha(1+k^2)^2+2\alpha^2+3(1+k^2)^3(1+3k^2)]$$
$$+(1+k^2)^2(3+9k^2+6k^4-2\alpha)\}. \tag{19}$$

We see that only the first contribution Q_0, related to self-interaction due to the zeroth harmonics, is angle dependent, while the latter two—respectively due to the cubic and quadratic terms in (equation (5c))—are *isotropic*. For parallel modulation, i.e. $\theta = 0$, the simplified expressions for $P|_{\theta=0}$ and $Q|_{\theta=0}$ are readily obtained from the above formulae; note that $P|_{\theta=0} < 0$, while $Q|_{\theta=0}$, even though positive for $k \to 0$ (see below), changes sign at some critical value of k.

A preliminary result regarding the behaviour of the coefficients P and Q for long wavelengths may be obtained by considering the limit of small $k \ll 1$ in the above formulae. The parallel ($\theta = 0$) and oblique ($\theta \neq 0$) modulation cases have to be distinguished straightaway. For small values of k ($k \ll 1$), P is negative and varies linearly as $P|_{\theta=0} \approx -3/2k$ in the parallel modulation case (i.e. $\theta = 0$), tending to zero for vanishing k, while for $\theta \neq 0$, P is positive and goes to infinity as $P|_{\theta\neq 0} \approx \sin^2\theta/(2k)$ for vanishing k. Therefore, the slightest deviation by θ of the amplitude variation direction with respect to the wave propagation direction results in a change in sign of the group-velocity dispersion coefficient P. On the other hand, Q varies as $\sim 1/k$ for small $k \ll 1$. For $\theta \neq 0$, Q is negative $Q|_{\theta\neq 0} \approx -(2\alpha-3)^2/(12k)$, while for vanishing θ, the approximate expression for Q changes sign, i.e. $Q|_{\theta=0} \approx +(2\alpha-3)^2/(12k)$; see that the well-known Hasegawa [17] result, i.e. $Q \sim 1/(3k)$, is recovered for $\alpha = 1/2$ (and $\theta = 0$). In conclusion, both P and Q change sign when 'switching on' *theta*. Since the wave's (linear) stability profile, expected to be influenced by obliqueness in modulation, essentially relies on (the sign of) the product PQ (see below), we see that long wavelengths will always be stable.

5. Linear stability analysis

The standard stability analysis consists in linearizing around the monochromatic wave solution of the NLSE (15): $\psi = \hat{\psi}\,\mathrm{e}^{\mathrm{i}Q|\hat{\psi}|^2\tau} + \text{c.c.}$ ('c.c.' denotes the complex conjugate; note the amplitude dependence of the frequency) by setting $\hat{\psi} = \hat{\psi}_0 + \epsilon\hat{\psi}_1$, and taking the perturbation $\hat{\psi}_1$ to be of the form: $\hat{\psi}_1 = \hat{\psi}_{1,0}\,\mathrm{e}^{\mathrm{i}(\hat{k}\zeta-\hat{\omega}\tau)} + \text{c.c.}$ (distinguish the perturbation wavenumber $\hat{k}$

and frequency $\hat{\omega}$ from the carrier wave quantities, k and ω). Substituting into (15), one obtains the dispersion relation

$$\hat{\omega}^2 = P^2\hat{k}^2\left(\hat{k}^2 - 2\frac{Q}{P}|\hat{\psi}_0|^2\right). \tag{20}$$

The wave will obviously be *stable* if the product PQ is negative. However, for positive $PQ > 0$, instability sets in for wavenumbers below a critical value $\hat{k}_{\rm cr} = \sqrt{2\frac{Q}{P}}|\hat{\psi}_0|$, i.e. for wavelengths above a wavelength threshold: $\lambda_{\rm cr} = 2\pi/\hat{k}_{\rm cr}$; defining the instability growth rate $\sigma = |{\rm Im}\,\hat{\omega}(\hat{k})|$, we see that it reaches its maximum value for $\hat{k} = \hat{k}_{\rm cr}/\sqrt{2}$, namely

$$\sigma_{\max} = |{\rm Im}\,\hat{\omega}|_{\hat{k}=\hat{k}_{\rm cr}/\sqrt{2}} = |Q||\hat{\psi}_0|^2. \tag{21}$$

We draw the conclusion that the instability condition depends only on the sign of the product PQ, which may now be studied numerically, relying on the exact expressions derived above.

In the contour plots presented below (see figures 1, 2), we have depicted the $PQ = 0$ boundary curve against the normalized wavenumber $k/k_{\rm D}$ (in abscissa) and angle θ (between 0 and π); the area in black/white represents the region in the (k–θ) plane where the product is negative/positive, i.e. where the wave is stable/unstable. We have considered values of the wavenumber k between zero and up to twice the Debye wavenumber $k_{\rm D}$ (yet mostly focusing our attention on the low k region). Angle θ is allowed to vary between zero and π (see that all plots are $\frac{\pi}{2}$ periodic).

First, as analytically predicted above, the product PQ is negative for small k, for all values of theta; long wavelengths will always be stable. For any given value of the modulation angle θ, instability sets in above a wavenumber threshold, say, $k_{\rm cr}$, which is clearly seen to decrease as the modulation angle θ increases from zero to approximately 30°, and then increases again up to $\theta \approx 60°$. Nevertheless, beyond that value (and up to $\pi/2$) the wave remains stable; this is even true for the wavenumber regions where the wave would be *unstable* to a parallel modulation. The inverse effect is also present: even though certain k values correspond to stability for $\theta = 0$, the same modes may become unstable when subject to an oblique modulation ($\theta \neq 0$). In all cases, the wave appears to be globally stable to large angle θ modulation (between 1 and $\pi/2$ radians, i.e. 60° to 90°).

It is interesting to trace the influence of the percentage of the minority cold electron population (related to $\nu = n_{\rm h}/n_{\rm c}$) on the qualitative remarks of the preceding paragraph. For a fixed value of the temperature ratio μ, we have numerically studied the sign of the PQ product on the k–θ plane, gradually increasing the cold component concentration (i.e. 'switching off' ν). A rather complex behaviour is witnessed in figures 1(a)–(d), due to the competition between the nonlinearity contributions $Q_{1,2}$ (angle dependent) and Q_0 (angle dependent). We see that a small presence of hot electrons ($\nu > 1$) may strongly modify the the wave's stability profile and even lead to instability in otherwise stable regions (cf figures 1(a)–(d)). Since the black/white regions in the figures correspond to dark/bright-type solitons (see below), we qualitatively deduce that a solitary wave of either type may become unstable while increasing the cold minority electron presence. For values of ν below unity ($n_{\rm h} < n_{\rm c}$), there seems to be no important effect on the wave's stability, as described above (cf figures 1(e), (f)). Intuitively speaking this is rather expected, since very low ($\nu \to 0$ i.e. $n_{\rm h} \ll n_{\rm c}$) and very high ($\nu \to \infty$ i.e. $n_{\rm h} \gg n_{\rm c}$) values of ν are identical in physical meaning: the ions are practically surrounded by a single-electron population (either c or h) at some temperature $T_{\rm e}$ ($> T_{\rm i}$). Note, in passing, that the well-known IAW previous result of $k_{\rm cr} = 1.47$ [25, 28] for the numerical solution of $PQ|_{\theta=0} = 0$ is exactly recovered here, for $\nu = 0$ (or $\nu \to \infty$) (see figure 1(a)).

On the other hand, keeping the value of the density ratio ν fixed ($\nu = 10$ in figure 2), we may carry out a similar study by gradually 'switching on' μ, i.e. decreasing the cold

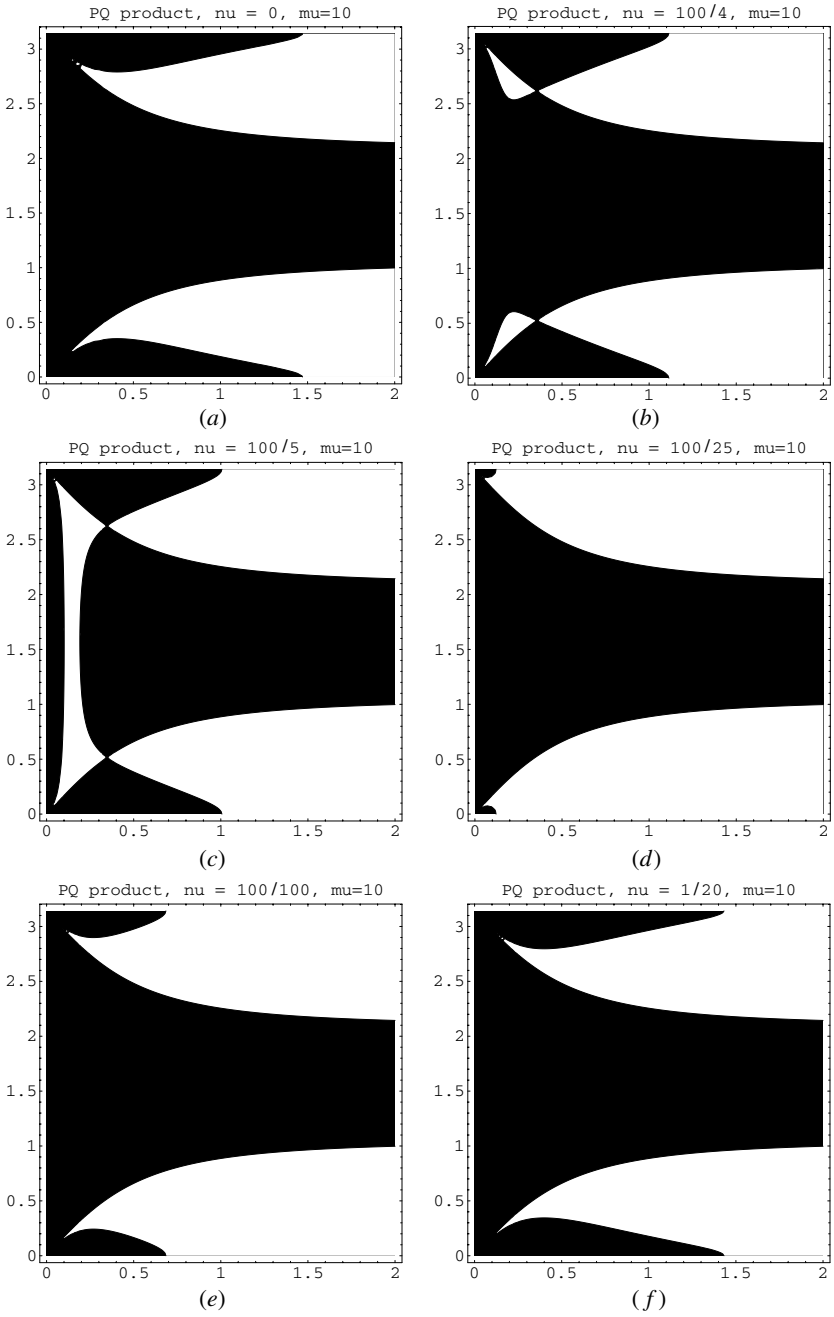

Figure 1. The $PQ = 0$ contour is depicted against normalized wavenumber k/k_{D} (in abscissa) and angle θ (between 0 and π); black/white represents the region where the product is negative/positive, i.e. the region of linear stability/instability which may support dark/bright-type solitary excitations. The electron temperature ratio $T_{\mathrm{h}}/T_{\mathrm{c}}$ is fixed at $\mu = 10$; several values of $\nu = n_{\mathrm{h}}/n_{\mathrm{c}}$ have been considered: (*a*) $\nu = 0$ (single-electron temperature IAW)—this is identical to $\nu \to \infty$; (*b*) $\nu = 25$ (hot electron presence dominant); (*c*) $\nu = 20$; (*d*) $\nu = 4$; (*e*) $\nu = 1$; (*f*) $\nu = 0.05$ (cold electrons dominant).

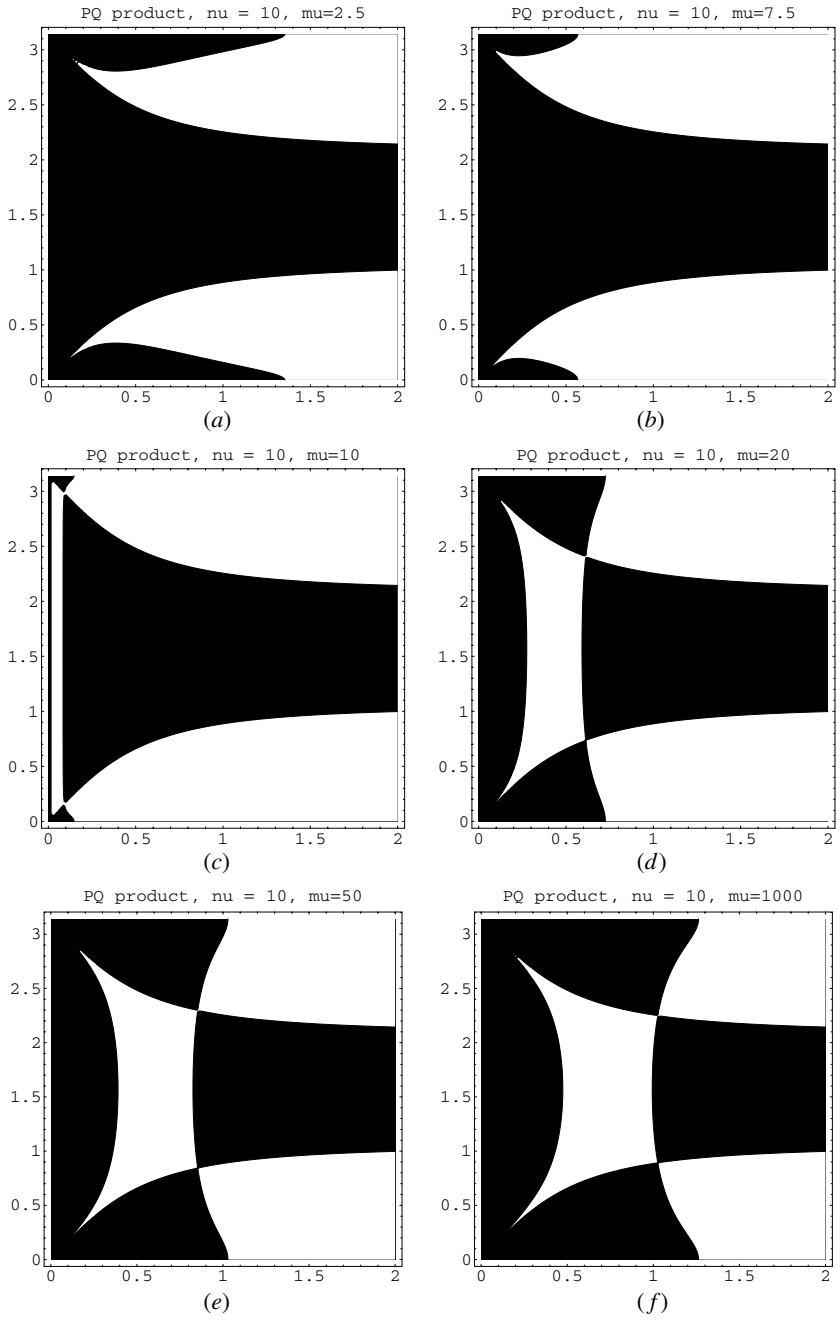

Figure 2. Similar to figure 1, for a (fixed) electron density ratio n_h/n_c of $\nu = 10$; several values of $\mu = T_h/T_c$ have been considered: (*a*) $\mu = 2.5$: only slightly different from the case $\mu = 1$ (or $\nu = 0$; cf figure 1); (*b*) $\mu = 7.5$; (*c*) $\mu = 10$; (*d*) $\mu = 20$; (*e*) $\mu = 50$; (*f*) $\mu = 1000$.

component temperature T_c. We see that low values of μ (see figures 2(*a*), (*b*)) are reminiscent of the ordinary (e–i) IAW (cf figure 1(*a*)), while for higher μ values (i.e. for a 'very cold' minority of cold electrons) new regions of instability appear at wide angles. Given that the sign

of PQ also affects the type of localized excitation supported by the plasma (see the following section), this suggests that a strong temperature difference between hot and cold electrons may destabilize dark excitations, in favour of bright envelope solitons. Nevertheless, a small temperature difference generally favours dark excitations, i.e. density voids accompanied by localized potential dips, in agreement with satellite observations [34].

6. Arbitrary amplitude nonlinear excitations

The NLSE (15) is known to possess distinct types of localized constant profile (solitary wave) solutions, depending on the sign of the product PQ. Remember that equation (15) describes the evolution of the wave's envelope, so these solutions represent slowly varying localized envelope structures, confining the (fast) carrier wave. Following [39], we may seek a solution of equation (15) in the form $\psi(\zeta,\tau) = \sqrt{\rho(\zeta,\tau)}\,\mathrm{e}^{\mathrm{i}\Theta(\zeta,\tau)}$, where ρ, σ are real variables which are determined by substituting into the NLSE and separating real and imaginary parts. The different types of solution thus obtained are summarized in the following.

For $PQ > 0$ we find the *(bright) envelope soliton*[3]

$$\rho = \rho_0 \operatorname{sech}^2\left(\frac{\zeta - u\tau}{L}\right) \qquad \Theta = \frac{1}{2P}\left[u\zeta - \left(\Omega + \frac{1}{2}u^2\right)\tau\right] \tag{22}$$

representing a localized pulse travelling at a speed u and oscillating at a frequency Ω (at rest). The pulse width L depends on the (constant) maximum amplitude square ρ_0 as $L = \sqrt{\frac{2P}{Q\rho_0}}$.

For $PQ < 0$ we have the *dark* envelope soliton (*hole*) [39]

$$\begin{aligned} \rho &= \rho_1\left[1 - \operatorname{sech}^2\left(\frac{\zeta - u\tau}{L'}\right)\right] = \rho_1 \tanh^2\left(\frac{\zeta - u\tau}{L'}\right) \\ \Theta &= \frac{1}{2P}\left[u\zeta - \left(\frac{1}{2}u^2 - 2PQ\rho_1\right)\tau\right] \end{aligned} \tag{23}$$

representing a localized region of negative wave density (shock) travelling at a speed u. Again, the pulse width depends on the maximum amplitude square ρ_1 via $L' = \sqrt{2\left|\frac{P}{Q\rho_1}\right|}$.

Finally, looking for velocity-dependent amplitude solutions, for $PQ < 0$, one obtains the *grey* envelope solitary wave [39]

$$\begin{aligned} \rho &= \rho_2\left[1 - a^2 \operatorname{sech}^2\left(\frac{\zeta - u\tau}{L''}\right)\right] \\ \Theta &= \frac{1}{2P}\left[V_0\zeta - \left(\frac{1}{2}V_0^2 - 2PQ\rho_2\right)\tau + \Theta_{10}\right] - S\sin^{-1}\frac{a\tanh\left(\frac{\zeta-u\tau}{L''}\right)}{\left[1 - a^2\operatorname{sech}^2\left(\frac{\zeta-u\tau}{L''}\right)\right]^{1/2}} \end{aligned} \tag{24}$$

which also represents a localized region of negative wave density; Θ_{10} is a constant phase; S denotes the product $S = \operatorname{sign} P \times \operatorname{sign}(u - V_0)$. In comparison to the dark soliton (23), note that apart from the maximum amplitude ρ_2, which is now finite (i.e. non-zero) everywhere, the pulse width of this grey-type excitation: $L'' = \sqrt{2\left|\frac{P}{Q\rho_2}\right|}\frac{1}{a}$, now also depends on a, given by: $a^2 = 1 + \frac{1}{2PQ}\frac{1}{\rho_2}\left(u^2 - V_0^2\right) \leqslant 1$ (for $PQ < 0$), an independent parameter representing the modulation depth ($0 < a \leqslant 1$). V_0 is an independent real constant which satisfies the condition [39]: $V_0 - \sqrt{2|PQ|\rho_2} \leqslant u \leqslant V_0 + \sqrt{2|PQ|\rho_2}$; for $V_0 = u$, we have $a = 1$ and thus recover the *dark* soliton presented in the previous paragraph.

[3] This result is immediately obtained from [39], by transforming the variables therein into our notation as follows: $x \to \zeta, s \to \tau, \rho_m \to \rho_0,\ \alpha \to 2P, q_0 \to -2PQ,\ \Delta \to L,\ E \to \Omega, V_0 \to u$.

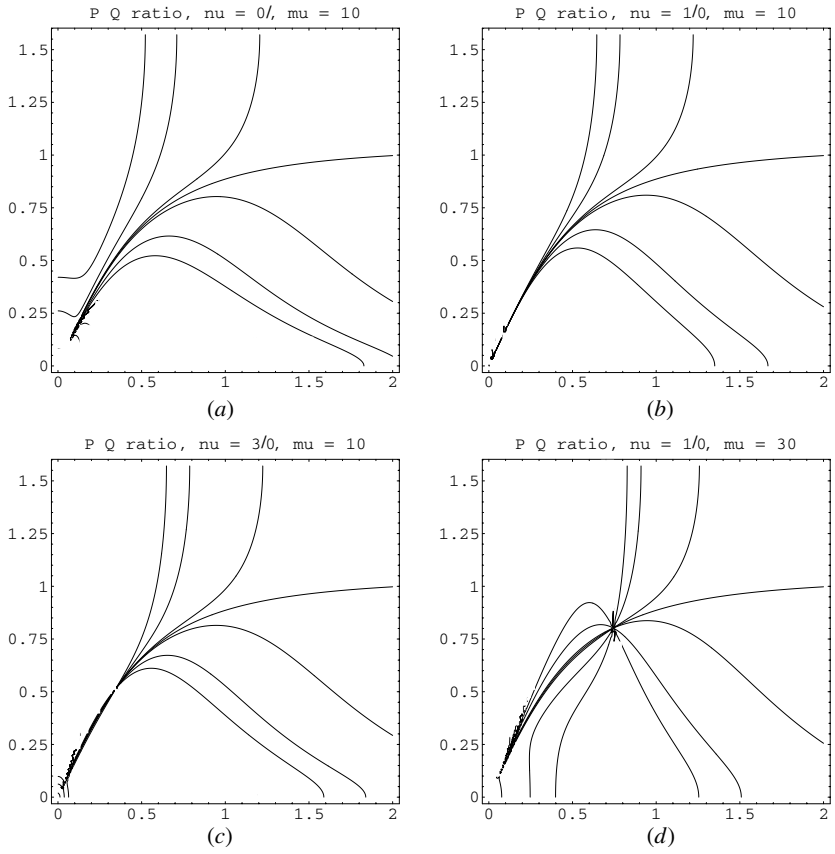

Figure 3. A few (normalized) soliton (square) width P/Q fixed value contours are depicted against (normalized) wavenumber k/k_{D} and modulation angle θ, for different electron density and temperature ratio (i.e. $\nu = n_{\mathrm{h}}/n_{\mathrm{c}}$ and $\mu = T_{\mathrm{h}}/T_{\mathrm{c}}$, respectively) pair values: (*a*) $\nu = 0$ (single-electron e–i plasma limit, for reference); (*b*) $\nu = 10, \mu = 10$; (*c*) $\nu = 30, \mu = 10$; (*d*) $\nu = 10, \mu = 30$. In descending order (from top to bottom), the contour values are: -0.25, -0.1, -0.01, 0, 0.01, 0.1 and 0.25.

We note that the envelope soliton width L will depend on the dispersion law via the P and Q coefficients, namely $L^2 \sim P/Q$ (see above); for instance, regions with higher values of P (or lower values of Q) will support wider (spatially more extended) localized excitations. The soliton width does not depend on the pulse velocity. It does, however, depend on parameters μ and ν, as suggested in figure 3. Upon careful inspection of figures 3(*b*), (*d*), we note that increasing the value of the temperature ratio μ (for a given value of ν) (cf figures 3(*b*), (*d*)) may result in narrower solitons for short wavelengths or even different soliton types for longer wavelengths. The inverse effect, yet less dramatic, is encountered when varying the value of the density ratio ν (for a given μ)—cf figures 3(*b*), (*c*): injecting cold electrons i.e. decreasing ν results in narrower solitary waves (pulses). We draw the qualitative conclusion that local variations of the cold component concentration may result in (either dark or bright) envelope wave (de)stabilization.

Summarizing, we have seen that the regions depicted in figures 1 and 2 actually also distinguish the regions where different types of localized solutions may exist: bright (dark or grey) solitons will occur in white (black) regions (the different types of NLS excitations are

exhaustively reviewed in [39]). Since, intuitively speaking, different directions of amplitude perturbation may coexist, for any given wavenumber, none of the above soliton types is *a priori* excluded at some given wave situation (nevertheless, long wavelengths mostly favour dark excitations (cf figures 1, 2)). Since a simultaneous propagation of nonlinear excitations (moving at different velocities and not interacting with each other) is in principle possible, the conjecture can be made that a local envelope soliton superposition may account for the apparent asymmetries observed in the potential and density variation structures reported by satellite observations. In particular, these results are in qualitative agreement with conclusions in [6], where it was argued that both compressive and rarefactive solitary structures may coexist, provided that the temperature difference is high enough.

7. Conclusions

This work has been devoted to the study of the modulation of ion-acoustic waves propagating in an unmagnetized plasma in the presence of two distinct thermalized electron populations. Allowing for modulation to occur in an oblique manner, we have shown that the conditions for modulational instability depend on the angle between the propagation and modulation directions. In fact, the region of parameter values where instability occurs is rather extended for angle θ values up to a certain threshold, and, in contrast, smeared out for higher θ values (and up to 90°, then going on in a $\frac{\pi}{2}$-periodic fashion).

Furthermore, we have studied the possibility of the formation of IAW-related localized structures (solitary waves) in the plasma. Distinct types of localized excitations (envelope solitons) have been shown to exist. Their type and propagation characteristics depend on the carrier wavenumber k and the modulation angle θ. These envelope excitations reproduce the qualitative features of localized structures (potential and density variations) observed by spacecraft and their study may provide a hint towards the explanation of the creation and persistence of the latter.

Acknowledgments

This work was supported by the European Commission (Brussels) through the Human Potential Research and Training Network for carrying out the task of the project entitled: 'Complex Plasmas: The Science of Laboratory Colloidal Plasmas and Mesospheric Charged Aerosols' through the contract no HPRN-CT-2000-00140.

References

[1] Krall N A and Trivelpiece A W 1973 *Principles of Plasma Physics* (New York: McGraw-Hill)
Stix Th 1992 *Waves in Plasmas* (New York: American Institute of Physics)
[2] Washimi H and Taniuti T 1966 *Phys. Rev. Lett.* **17** 996
[3] Tajiri M and Nishihara K 1984 *J. Phys. Soc. Japan* **54** 572
Chakraborty D and Das K P 2003 *Phys. Plasmas* **10** 2236
[4] Sagdeev R Z 1966 *Reviews of Plasma Physics* vol 4 ed M A Leontovich (New York: Consultants Bureau) p 52
[5] Buti B 1980 *Phys. Lett.* A **76** 251
[6] Nishihara H and Tajiri M 1981 *J. Phys. Soc. Japan* **50** 4047
[7] Ghosh S S *et al* 1996 *Phys. Plasmas* **3** 3939
[8] Ikezi H 1970 *Phys. Rev. Lett.* **25** 11
Nakamura Y *et al* 1985 *J. Plasma Phys.* **33** 237
Nakamura Y and Tsukabayashi I 1985 *J. Plasma Phys.* **34** 401
[9] Akhmediev N and Soto-Crespo J M 1993 *Phys. Rev.* A **47** 1358
[10] Boardman A D *et al* 2000 *Phys. Rev.* A **62** 2871

[11] Agrawal G P 1987 *Phys. Rev. Lett.* **59** 880
Potasek M J and Agrawal G P 1987 *Phys. Rev.* A **36** 3862
[12] Buryak A V and Kivshar Yu S 1995 *Phys. Lett.* A **197** 407
Trillo S, Buryak A V and Kivshar Yu S 1996 *Opt. Commun.* **122** 200
also see Buryak A V *et al* 2002 *Phys. Lett.* A **370** 63 (for a recent review)
[13] Hasegawa A 1989 *Optical Solitons in Fibers* (Berlin: Springer)
[14] Agrawal G 2001 *Nonlinear Fiber Optics* (New York: Academic)
[15] Kivshar Yu S and Peyrard M 1992 *Phys. Rev.* A **46** 3198
Daumont I, Dauxois T and Peyrard M 1997 *Nonlinearity* **10** 617
[16] Remoissenet M 1994 *Waves Called Solitons* (Berlin: Springer)
[17] Hasegawa A 1975 *Plasma Instabilities and Nonlinear Effects* (Berlin: Springer)
[18] Shukla P K, Stenflo L and Fedele R 2001 *Phys. Scr.* **64** 553
[19] Theocharis G *et al* 2003 *Phys. Rev.* A **67** 063610
[20] Bilbault J M, Marquié P and Michaux B 1995 *Phys. Rev.* E **51** 817 (also see in [16])
[21] Agrawal G 2002 *Fiber Optic Communication Systems* (New York: Wiley)
[22] Davydov A S 1985 *Solitons in Molecular Systems* (Dordrecht: Kluwer)
[23] Taniuti T and Yajima N 1969 *J. Math. Phys.* **10** 1369
Asano N, Taniuti T and Yajima N 1969 *J. Math. Phys.* **10** 2020
[24] Sulem P and Sulem C 1999 *Nonlinear Schrödinger Equation* (Berlin: Springer)
[25] Shimizu K and Ichikawa H 1972 *J. Phys. Soc. Japan* **33** 789
[26] Kakutani T and Sugimoto N 1974 *Phys. Fluids* **17** 1617
Kako M 1974 *Prog. Theor. Phys. Suppl.* **55** 1974
[27] Chan V and Seshadri S 1975 *Phys. Fluids* **18** 1294
Durrani I *et al* 1979 *Phys. Fluids* **22** 791
Sharma S R *et al* 1978 *Phys. Lett.* A **68** 54
Xue J-K, Duan W-S and He L 2002 *Chin. Phys.* **11** 1184
[28] Kako M and Hasegawa A 1976 *Phys. Fluids* **19** 1967
Chhabra R and Sharma S 1986 *Phys. Fluids* **29** 128
Mishra M, Chhabra R and Sharma S 1994 *Phys. Plasmas* **1** 70
[29] Ichikawa Y H, Imamura T and Taniuti T 1972 *J. Phys. Soc. Japan* **33** 189
Sanuki H, Shimizu K and Todoroki J 1972 *J. Phys. Soc. Japan* **33** 198
Ichikawa Y H and Taniuti T 1973 *J. Phys. Soc. Japan* **34** 513
[30] Watanabe S 1977 *J. Plasma Phys.* **17** 487
[31] Jones W D 1975 *Phys. Rev. Lett.* **35** 1349
[32] Berthomier M *et al* 1968 *J. Geophys. Res.* **103** 4261
[33] Nishida Y and Nagasawa T 1986 *Phys. Fluids* **29** 345
[34] Ergun R E *et al* 1998 *Geophys. Res. Lett.* **25** 2061
Delory G T *et al* 1998 *Geophys. Res. Lett.* **25** 2069
Pottelette R *et al* 1999 *Geophys. Res. Lett.* **26** 2629
[35] McFadden J P *et al* 2003 *J. Geophys. Res.* **108** 8018
[36] Temerin M 1982 *Phys. Rev. Lett.* **48** 1175
[37] Boström R 1988 *Phys. Rev. Lett.* **61** 82
[38] Matsumoto H *et al* 1994 *Geophys. Res. Lett.* **21** 2915
Franz J R *et al* 1998 *Geophys. Res. Lett.* **25** 1277
Cattell C A *et al* 1999 *Geophys. Res. Lett.* **26** 425
[39] Fedele R *et al* 2002 *Phys. Scr.* T **98** 18
Fedele R and Schamel H 2002 *Eur. Phys. J.* B **27** 313